# Cooley-Tukey FFT Algorithm based on GDFT for Phasor Estimation by PMU under Power Quality Disturbances

**Mohamed Abbaci**
Laboratory of Advanced Electronic Systems (LSEA), University of Medea, Algeria | PTAPC Ouargla, CRAPC, Algeria
abbaci.mohamed@crapc.dz
(corresponding author)

**Mohamed Ould Zmirli**
Laboratory of Advanced Electronic Systems (LSEA), University of Medea, Algeria
m_zmirli@yahoo.fr

*Received: 30 September 2022 | Revised: 13 November 2022 | Accepted: 19 November 2022*

**ABSTRACT**

**Due to the high penetration of renewable energy sources, such as photovoltaic panels and wind turbines, in addition to the use of different electric power supplies in the power grid, there are major disturbances in the forms of electric waves. These variations and disturbances must be monitored and controlled for the efficient management of transmission and distribution of electrical energy, safety, and electrical protection systems. Nowadays, Phasor Measurement Unit (PMU) technology is an essential tool to develop the supervision, protection, and control of the electrical power grid. PMUs measure the amplitude and angle of current and voltage waveforms on a Coordinated Universal Time (UTC) time scale and speedily measure the fundamental frequencies and their rates of change using fast and accurate estimation algorithms. This paper presents a phasor estimation using a Modified Cooley-Tukey Fast Fourier Transform algorithm based on the Generalized Discrete Fourier Transform (DFT) used in PMUs, using simulations in MATLAB. This algorithm was utilized to accelerate and simplify the computation of DFTs. To validate the performance under waveform disturbances, several tests with different waveforms and disturbances were simulated and interpreted according to the standard and compared with DFT.**

***Keywords-phasor measurement unit; rate of change of frequency; total vector error; DFT; GDFT; CTGDFT***

## I. INTRODUCTION

Phasor Measurement Units (PMUs) are widely used for many years in electrical systems for control and monitoring, with accurate and fast fundamental component measurements [1, 2]. The phasor estimation is the main component of a PMU [3], so DFT is the most widely used algorithm [1, 4]. PMUs were introduced in response to the need for more efficient and secure monitoring devices in power grids. Since the developments in synchronized measurement technology, wide-area measurement systems are suitable to follow the dynamic behavior of electrical power systems using PMUs and PDC hierarchically [5, 6]. PMUs precisely measure the amplitudes and phase angles of the waveforms of the electrical network (current, voltage, and frequency) at various points [7, 8] using time stamping. Measured and calculated data are transmitted through a synchronized GPS transmission medium to a PDC [9]. Information from multiple PMUs located throughout the electrical power system is analyzed and processed at the PDC to detect electrical disturbances [10] and improve the protection and control functions of an electric power system [6]. The IEEE 1344-1995 was the first published standard for conventions relating to original synchrophasor measurements [11, 12]. In 2005, IEEE C37.118-2005 was introduced and replaced the existing synchrophasor standard [1, 12]. In 2011, two new standards were published to address the measurement requirement (IEEE C37.118.1-2011) and synchrophasor communications (IEEE C37.118.2-2011 ) [11, 13, 14].

This study investigated the modified Cooley-Tukey Fast Fourier Transform (FFT) algorithm, based on a Generalized Discrete Fourier Transform (GDFT) framework, for PMU phasor estimation. The conventional Cooley-Tukey algorithm accelerates and simplifies the DFT calculation, but has disadvantages such as slow dynamics and sensitivity to frequency variations. The use of the Cooley-Tukey FFT algorithm based on the GDFT was proposed in [15] to overcome these drawbacks. Simulations were carried out to highlight the performance of the suggested algorithm over standard DFT techniques.

## II. PHASOR MEASUREMENT ARCHITECTURES

### A. Block Diagram of PMU

The functional diagrams of PMUs may differ from one manufacturer to another. Figure 1 shows a basic block diagram of a PMU [13]. A PMU generally consists of three main blocks: measurement, calculation, and communication [16].

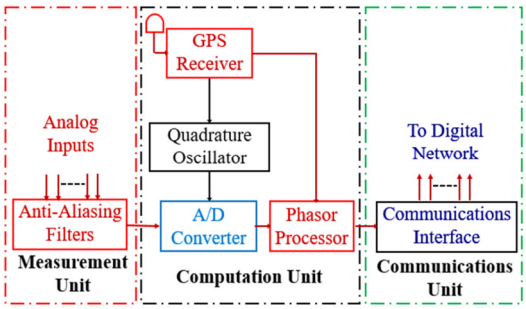


Fig. 1. Phasor Measurement Unit Components.

- The Measurement Unit receives analog data inputs such as three-phase voltages, three-phases, and neutral currents from the secondary measurement transformers (VT and CT), which are later filtered to eliminate and prevent aliasing errors by antialiasing filters [13, 17].
- The Computation Unit includes Analog-to-Digital Converters (A/D), Quadrature Oscillator, and Phasor Processor [18, 20].
- The computed synchrophasor and other information are transmitted to the PDC to be interchanged between other PMUs for monitoring, control applications, and system protection using communication units [13, 16].

### B. Wide Area Measurement Systems

The Wide Area Monitoring System (WAMS) collects real-time information on the status of the network at strategic points, with precise time stamping by GPS satellites. WAMS improves network analysis, integrating PMUs to detect any instability. The WAMS uses synchronized measurement data and modern communication systems to supervise, monitor, and analyze the current state of the wide-area power system and serves for the operation, control, and protection of the power system in real-time [18, 19]. WAMS systems mainly consist of three components [13]: Phasor Measurement Unit, Communication network, and Phasor Data Concentrator.

#### 1) Phasor Measurement Unit (PMU)

The PMU is a measuring device for electrical power systems, capable of performing phasor measurements of voltages and currents in large and distributed power system networks. The voltage and current waveforms of the power system are sinusoidal. A sinusoidal waveform is written as:

$$x(t) = X_m \cos(2\pi f t + \varphi) \quad (1)$$

where $X_m$ is the amplitude, $f$ is the frequency, $\varphi$ is the angle, and $t$ is the time. The representation of the phasor in the complex plane is:

$$X = \frac{X_m}{\sqrt{2}} e^{j\varphi} \quad (2)$$

$$X = \frac{X_m}{\sqrt{2}} (\cos\varphi + j \sin\varphi) = X_r + jX_i \quad (3)$$

where $X_r$ and $X_i$ are the real and the imaginary components of the complex form, and $\frac{X_m}{\sqrt{2}}$ is the RMS value. Figure 2 shows the phasor representation of a sinusoidal input signal at the angular frequency in the complex plane [10, 17]. In the case of a phase current or voltage, the projection of the phase vector on the ordinate axis (imaginary axis) gives the value of the current or voltage at that instant.

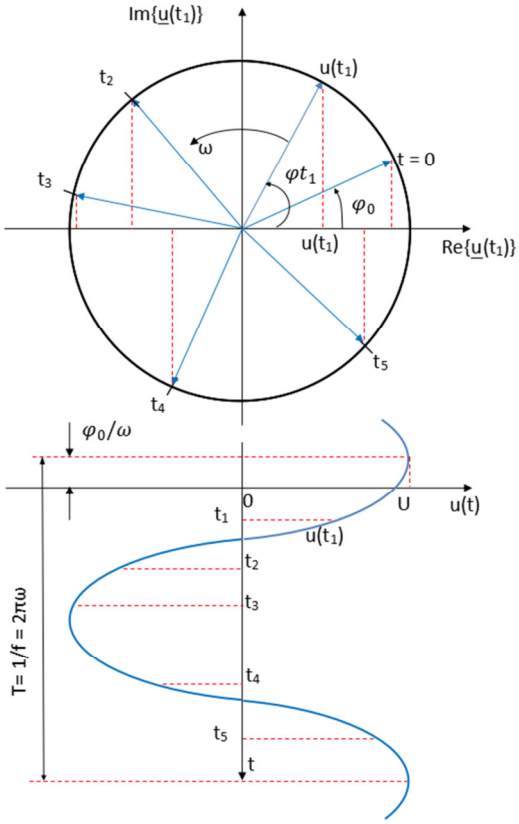


Fig. 2. Phasor representation of a sinusoidal signal.

#### 2) Communication Network

PMUs are usually located in substations that are geographically distant from the PDC. Communication networks are required to transmit information and measurements collected by PMUs from the substations to the control center [18]. Power grid monitoring and control require a high-speed communication framework that allows reliable, secure, and fast sharing of synchronized monitoring data between PMUs and PDC.

#### 3) Phasor Data Concentrator

Figure 3 shows the implementation of PDCs in a wide area monitoring system. The PDC collects discrete events and phasor data from PMUs, and probably other PDCs, and transmits them to other applications via a communications

protocol [10, 21]. Depending on the location of the PMU, the communication link between the PMU and the PDC may be a wired connection, a serial or Ethernet cable, or a wireless link.

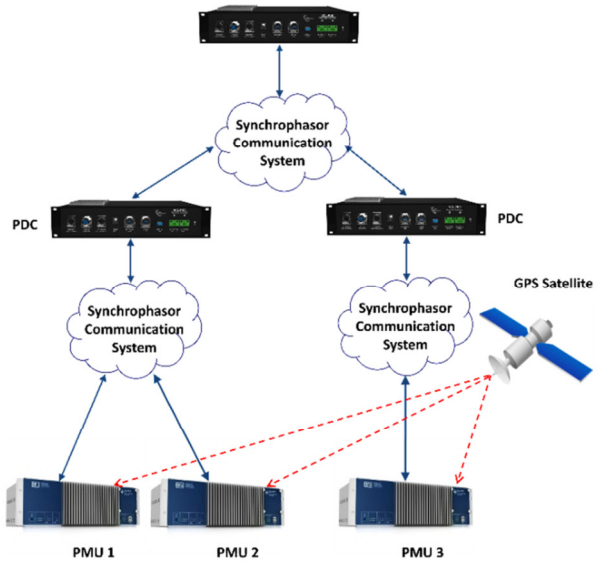


Fig. 3. Implementation of PDCs in WAMS.

Each PMU has two communication interfaces: One interface for communication of the PMUs via IEEE C37.118 and another to communicate with the digital control system. The central evaluation system collects the data, archives them, and displays them on a graphical user interface. This system can also be used to automatically monitor the electrical system and redistribute information to other PDCs or a numerical control system [10]. Communication of PMUs with PDCs, according to the IEEE C37.118 standard, is a client-server communication in which the PDC works as a client and the PMU as a server [10, 22].

## III. PERFORMANCE INDICES OF MEASUREMENT EVALUATIONS

### A. Total Vector Error (TVE)

C37.118.1-2011 defines the total vector error to calculate the phasor estimation error and to evaluate the performance of the phasor estimation. TVE compares the theoretical value of an input signal with its estimated value at the same time [10]. TVE is calculated by considering the error of estimating the amplitude and phase angle [13]. The TVE at time *n* is defined as :

$$TVE(n) = \sqrt{\frac{\left(\hat{X}_r(n)-X_r(n)\right)^2+\left(\hat{X}_i(n)-X_i(n)\right)^2}{\left(X_r(n)\right)^2+\left(X_i(n)\right)^2}} \quad (4)$$

where $\hat{X}_r(n)$ and $\hat{X}_i(n)$ are the real and the imaginary components of the estimated phasor, and $X_r(n)$ and $X_i(n)$ are the theoretical values at time $(n)$. Figure 4 shows the TVE representation.

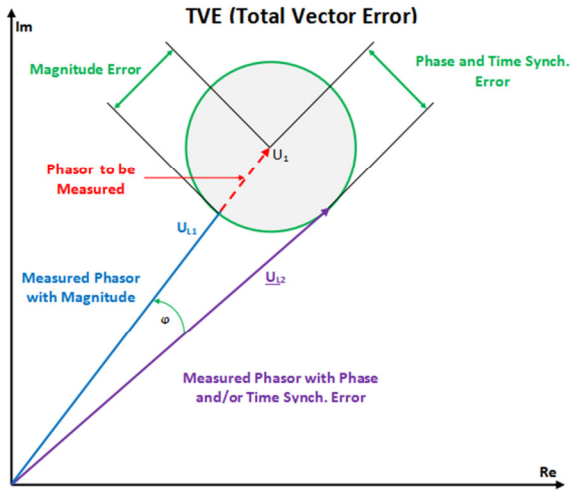


Fig. 4. Calculation of TVE.

### B. Frequency Error

In addition to the synchrophasor, PMUs also calculate the power system's frequency. Frequency Error (FE) is the difference between the estimated and the theoretical frequency. The sinusoidal signal of (1) may be written as [18]:

$$x(t) = X_m \cos\left(\theta(t)\right) \quad (5)$$

The frequency of the signal (5) is determined as:

$$f(t) = \frac{1}{2\pi}\left(\frac{d\theta(t)}{dt}\right) \quad (6)$$

FE is defined as:

$$FE = \left|f - \hat{f}\right| \quad (7)$$

### C. Rate Of Change Of Frequency Error (RFE)

ROCOF, measured by PMU at a given time instant, is determined by:

$$ROCOF(t) = \frac{d\left(\frac{1}{2\pi}\frac{d\theta(t)}{dt}\right)}{dt} = \frac{df(t)}{dt} \quad (8)$$

RFE is the difference between the theoretical and the estimated ROCOF value at a particular time instant [11]:

$$RFE = \left|\left(\frac{df}{dt}\right) - \left(\frac{\widehat{df}}{dt}\right)\right| \quad (9)$$

## IV. PMU ESTIMATION ALGORITHMS

Most phasor estimation algorithms utilized in commercial PMUs depend on the DFT estimation technique. The IEEE C37.118 standard does not recommend the use of a special algorithm or measurement in the PMU. Consequently, various estimation methods and algorithms are used in PMUs [12].

### A. DFT Algorithm

A sinusoidal waveform $x(t)$ of $kf_0$ frequency with a Fourier series can be written as:

$$x(t) = a_k \cos(2\pi k f_0 t) + b_k \sin(2\pi k f_0 t) \quad (10)$$

$$x(t) = \left\{\sqrt{(a_k^2 + b_k^2)}\right\} \cos(2\pi k f_0 t + \emptyset) \quad (11)$$

where $\emptyset = tan^{-1}(-b_k/a_k)$ . The phasor representation becomes:

$$X_K = \frac{1}{\sqrt{2}}\left\{\sqrt{(a_k^2 + b_k^2)}\right\}e^{j\emptyset} \quad (12)$$

and the complex form of the phasor becomes:

$$X_K = \frac{1}{\sqrt{2}}(a_k - jb_k) \quad (13)$$

By applying the relationship of the Fourier series coefficients, the phasor formula is determined by:

$$X_K = \frac{1}{\sqrt{2}}\frac{2}{N}\sum_{n=0}^{N-1} x_n\, e^{-\frac{j2\pi kn}{N}} \quad (14)$$

and also:

$$X_K = \frac{\sqrt{2}}{N}\sum_{n=0}^{N-1} x_n \left\{cos\left(\frac{2\pi kn}{N}\right) - j\, sin\left(\frac{2\pi kn}{N}\right)\right\} \quad (15)$$

where $N$ is the number of samples, $x_n$ is the input signal, $n$ is the sample number and $k$ is the harmonic index.

$$X_r = \frac{\sqrt{2}}{N}\sum_{n=0}^{N-1} x_n\, cos\left(\frac{2\pi kn}{N}\right) \quad (16)$$

$$X_i = \frac{\sqrt{2}}{N}\sum_{n=0}^{N-1} x_n\, sin\left(\frac{2\pi kn}{N}\right) \quad (17)$$

The phasor $X_k$ becomes:

$$X_k = X_r + jX_i \quad (18)$$

The phasor magnitude of the phasor is given by:

$$|X_k| = \sqrt{{X_r}^2 + j{X_i}^2} \quad (19)$$

And finally, the phase angle of the phasor is defined by:

$$\emptyset = tan^{-1}\frac{X_i}{X_r} \quad (20)$$

### *B. Proposed Algorithm*

This study investigated the Cooley-Tukey FFT algorithm, based on a Generalized DFT (CTGDFT), for phasor estimation. GDFT is described by:

$$X_k = \sum_{n=0}^{N-1} \omega_N^{(n+a)(k+b)}\, x_n \quad (21)$$

where $\omega_N = e^{-\frac{2\pi i}{N}}$, and $a$ and $b$ are two arbitrary complex numbers ($a = b = 0$ gives the ordinary DFT) [23]. The second transform is presented by the Cooley-Tukey FFT algorithm to accelerate and simplify the computation of DFTs [24, 25]. This algorithm is based on the factorization of $N$, the length of the DFT as a product of a number less than $N$. Supposing that $N$ is not a prime number, it is possible to write it as $N = N_1N_2$, where the two factors are greater than 1. The DFT formula is:

$$X_K = \sum_{n=0}^{N-1} x_n\, e^{-\frac{j2\pi kn}{N}} \quad (22)$$

This algorithm begins by dividing the range of integers from 0 to $N$-1 in two different ways. For time index $n$ or frequency index $k$, the division is divided into $N_1$ intervals of $N_2$ length each. The variables $n$ and $k$ are expressed as:

$$\begin{cases} n = n_1 + n_2N_1; 0 \le n_1 \le N_1 - 1; 0 \le n_2 \le N_2 - 1 \\ k = k_1N_2 + k_2; 0 \le k_1 \le N_1 - 1; 0 \le k_2 \le N_2 - 1 \end{cases} \quad (23)$$

The DFT Formula can be written in terms of $n_1$, $n_2$, $k_1$, $k_2$ as:

$$X_{k_1N_2+k_2} = \sum_{n_1=0}^{N_1-1}\sum_{n_2=0}^{N_2-1} x_{n_1+n_2N_1} e^{-\frac{j2\pi(n_1+n_2N_1)(k_1N_2+k_2)}{N}} \quad (24)$$

So, also:

$$X_{k_1N_2+k_2} = \sum_{n_1=0}^{N_1-1} \omega_{N_1}^{n_1k_1}\, \omega_N^{n_1k_2} \sum_{n_2=0}^{N_2-1} x_{n_1+n_2N_1}\, \omega_{N_2}^{n_2k_2} \quad (25)$$

where $\omega_N = e^{-\frac{j2\pi}{N}}$, $\omega_{N_1} = e^{-\frac{j2\pi}{N_1}}$, and $\omega_{N_2} = e^{-\frac{j2\pi}{N_2}}$. The inner summation was reduced to a standard DFT of $N_2$ size. Furthermore, the splitting of the first exponential into two factors unveils that the outer summation is also a standard DFT of $N_1$ size, of the product of the DFT of $N_2$ size multiplied by the twiddle factors. Applying the composition $N=N_1N_2$, the Cooley-Tukey re-indexings $n_1+n_2N_1$ and $k_1N_2+k_2$ can be used in (21). Then, the formula utilized in the modified Cooley-Tukey FFT algorithm based on GDFT is given by:

$$X_k = \omega_N^{ka} \sum_{n_1=0}^{N_1-1} \omega_{N_1}^{n_1k_1}\, \omega_N^{n_1k_2} \left(\sum_{n_2=0}^{N_2-1} x_n \omega_{N_2}^{n_2k_2}\, \omega_N^{nb}\right) \quad (26)$$

where $k=k_1N_2+k_2$ and $n=n_1+n_2N_1$.

## V. SIMULATION RESULTS OF DISTURBANCE FAULTS

### *A. Simulation Parameters*

The selected simulation parameters were:

- Nominal frequency: $f_0$ = 50Hz
- Number of samples: 400 samples/cycle
- Sample rate: 20kHz

The input signal is generated from a two-phase voltage (line voltage) of a secondary Potential Transformer ($U_{RMS}$ = 100V) with a cosinusoidal form, i.e. the phase AB.

### *B. Disturbance Faults and Evaluation Performance*

To evaluate the operation reliability of the PMU, different disturbance faults should be examined with the application of the proposed algorithm. As the performance and evaluation of PMUs are tested under disturbed power system conditions, 3 different disturbance faults were examined. For each case, voltage input signal, phasor magnitude, phasor angle, TVE, estimated frequency, and ROCOF were simulated. This paper shows only the simulation results of the TVE and the estimated frequency to evaluate the performance of the PMU. The frequency is estimated according to (6) and tracking is carried out by iterative DFT with re-sampling, as presented in [26], with a modification in the first cycle of frequency calculation (3 phasors are calculated in the first cycle to obtain the measured frequency). The simulation results of the disturbance faults were as follows:

#### *1) Disturbance Faults 1*

The idea of this steady-state test was to examine the effect of the input signal magnitude variations and its phase angle around its nominal values while keeping the frequency constant. This test signal was then generated with a modified magnitude of ±20% of the nominal and a phase angle of 45°, as in [27], at $t_1$= 0.2s and $t_2$= 0.5s:

$$v(t) = 80\sqrt{2}\,cos(2\pi f + \pi/4) \quad (27)$$

In the first disturbance fault, a variation of amplitude and phase were introduced to the voltage input signal. Figure 5 shows that the amplitude and phase values measured by the PMU were identical to the theoretical values, the evaluation parameters were in the norms, and TVE was almost 0%. Table I shows that the maximum value of the Frequency Error (FE) of the proposed algorithm was 0.0003Hz.

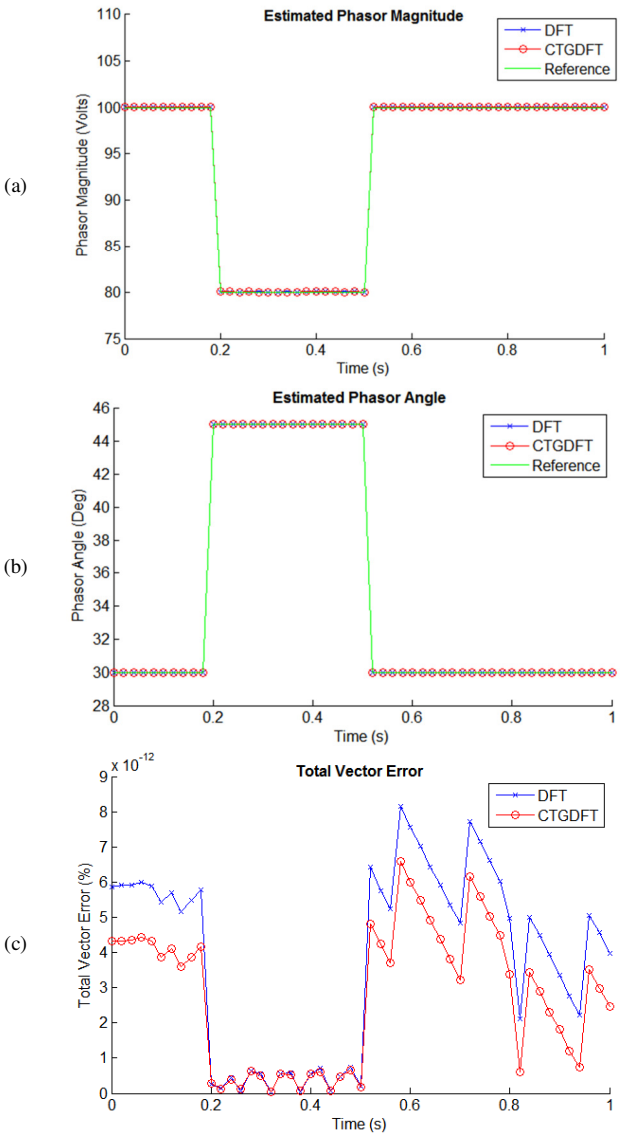


Fig. 5. Simulation results under Disturbance Faults 1: (a) estimated phasor magnitude, (b) estimated phasor angle, (c) total vector error.

TABLE I. ESTIMATED FREQUENCY, FREQUENCY ERROR, AND ROCOF ERROR UNDER DISTURBANCE FAULTS 1

| Method | Frequency (Hz) | | FE (Hz) | RFE (Hz/s) |
|---|---|---|---|---|
| | Min | Max | | |
| **DFT** | 50 | 50 | 0 | 0.00002 |
| **CTGDFT** | 49.9997 | 50 | 0.0003 | 0.00034 |

*2) Disturbance Faults 2*

This test examined the variation of the magnitude of the voltage input signal when the input signal frequency is 45Hz:

$$v(t) = 80\sqrt{2}\,cos(2\pi f + \pi/6) \quad (28)$$

Figure 6 shows the efficiency of the results obtained. Table II shows that the maximum FE was on the order of 0.0003Hz.

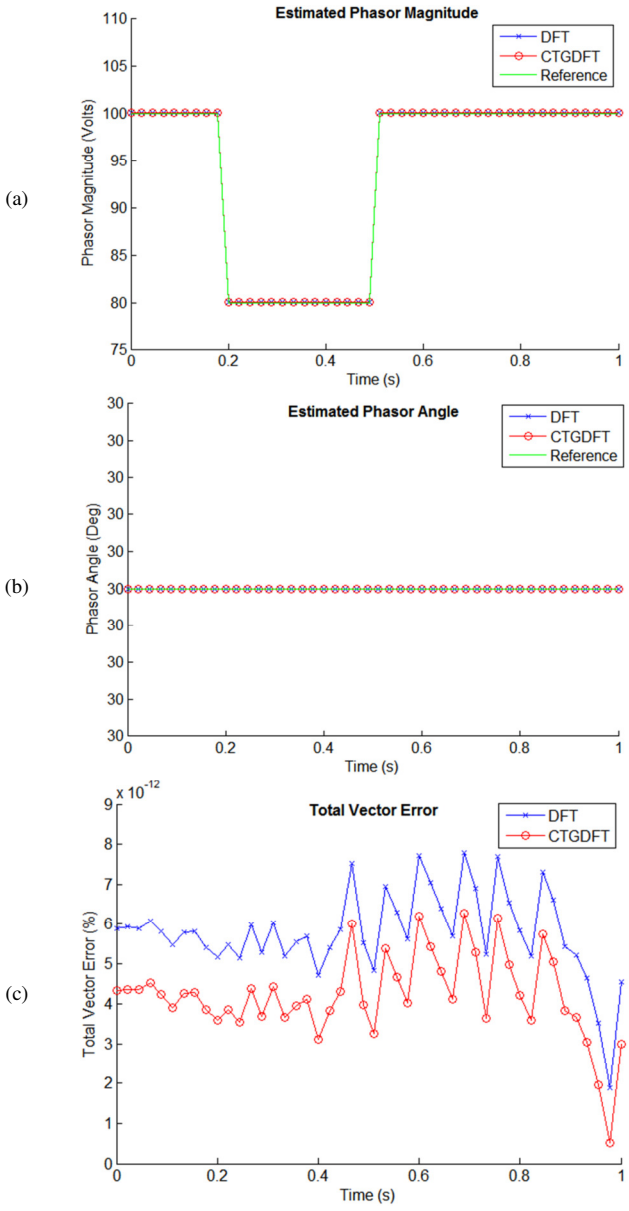


Fig. 6. Simulation results under Disturbance Faults 2: (a) estimated phasor magnitude, (b) estimated phasor angle, (c) total vector error.

TABLE II. ESTIMATED FREQUENCY, FREQUENCY ERROR, AND ROCOF ERROR UNDER DISTURBANCE FAULTS 2

| Method | Frequency (Hz) | | FE (Hz) | RFE (Hz/s) |
|---|---|---|---|---|
| | Min | Max | | |
| **DFT** | 45 | 45 | 0 | 0.00002 |
| **CTGDFT** | 44.9997 | 45 | 0.0003 | 0.00034 |

*3) Disturbance Faults 3*

Standard harmonic distortion tests require signals with 10% harmonics ranging from the second to the 50th harmonic. In this last test, only test signals containing 10% of the third and fifth harmonic components were generated, and a random noise was introduced into the voltage input signal with a slight variation in amplitude (-5%) and angle (+2°) at the $t$= 0.2s:

$$v(t) = 95\sqrt{2}\,cos(2\pi f + \pi/5.625) + 10\sqrt{2}\,cos(6\pi f + \pi/3) + 10\sqrt{2}\,cos(10\pi f + 5\pi/6) + e(t) \quad (29)$$

where $e(t)$ is the random noise. When the voltage input signal is superposed on a set of the third and fifth harmonic components and random noise with amplitude and phase variations, TVE was less than 0.15%, as shown in Figure 7.

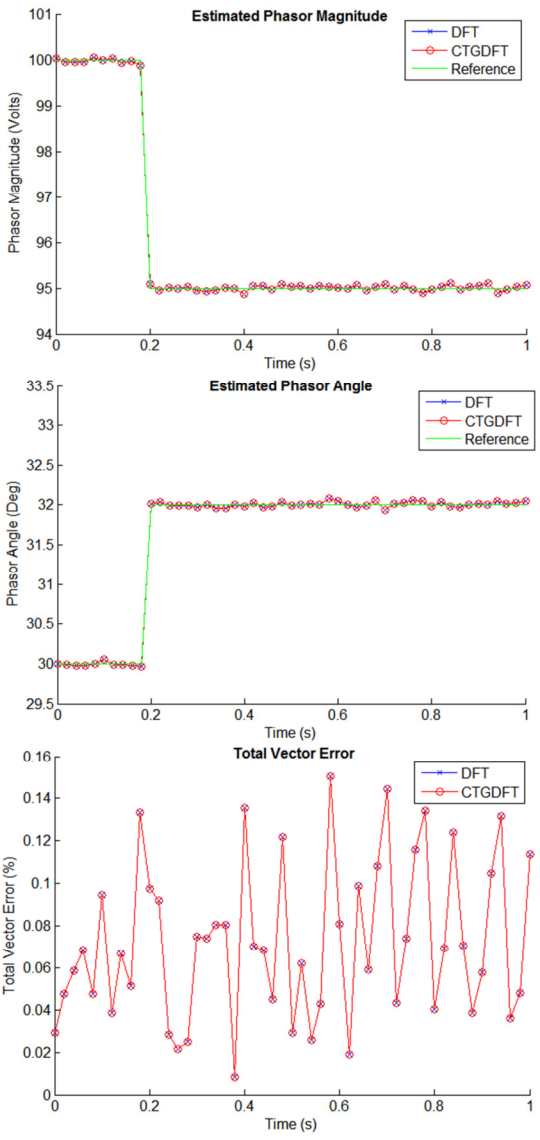


Fig. 7. Simulation results under Disturbance Faults 3: (a) estimated phasor magnitude, (b) estimated phasor angle, (c) total vector error.

Table III shows that the maximum FE of the proposed method was again in the order of 0.0003Hz.

TABLE III. ESTIMATED FREQUENCY, FREQUENCY ERROR, AND ROCOF ERROR UNDER DISTURBANCE FAULTS 3

| Method | Frequency (Hz) | | FE (Hz) | RFE (Hz/s) |
|---|---|---|---|---|
| | Min | Max | | |
| **DFT** | 49.9995 | 50 | 0.0005 | 0.00047 |
| **CTGDFT** | 49.9997 | 50 | 0.0003 | 0.00026 |

The IEEE C37.118.1-2011 standard specifies a TVE limit of 1%, an FE limit of 0.005Hz, and a limit of 0.01Hz/s for the ROCOF Error (RFE). The obtained TVE and FE limits were 0.15% and 0.0003Hz, respectively.

## VI. CONCLUSION

This study investigated the performance of the proposed Cooley-Tukey FFT algorithm based on GDFT for phasor estimation under conditions of power system disturbance. The performance of a PMU was examined and simulated by applying a voltage signal in different case studies. The performance and the evaluation of the results were analyzed according to the PMU standard (IEEE C37.118.1-2011) by calculating performance indices like TVE, Frequency Error (FE), and ROCOF Error (RFE). The performance of the proposed algorithm was tested under static and dynamic power system conditions, which is important for protection relay applications. The results obtained by the proposed method showed that the measurement evaluation parameters and PMU performance under power system disturbance conditions, such as integer harmonics component, frequency variation, input signal variation (amplitude and phase), and noise conditions, were in the limits according to the PMU standard (IEEE C37.118.1-2011). It should also be noted that the results of the PMU tests were very encouraging. Future work could investigate the implementation of the proposed algorithm in an embedded system as part of a PMU architecture.

## REFERENCES

[1] R. B. Sharma and G. M. Dhole, "Wide Area Measurement Technology in Power Systems," *Procedia Technology*, vol. 25, pp. 718–725, Jan. 2016, https://doi.org/10.1016/j.protcy.2016.08.165.

[2] S. Priyadarshini and C. K. Panigrahi, "Optimal Allocation of Synchrophasor Units in the Distribution Network Considering Maximum Redundancy," *Engineering, Technology & Applied Science Research*, vol. 10, no. 6, pp. 6494–6499, Dec. 2020, https://doi.org/10.48084/etasr.3862.

[3] P. Nanda, C. K. Panigrahi, and A. Dasgupta, "Phasor Estimation and Modelling Techniques of PMU- A Review," *Energy Procedia*, vol. 109, pp. 64–77, Mar. 2017, https://doi.org/10.1016/j.egypro.2017.03.052.

[4] P. R. Bedse and N. N. Jangle, "Review on PMU using Recursive DFT Algorithm," in *2018 International Conference on Computing, Power and Communication Technologies (GUCON)*, Sep. 2018, pp. 375–377, https://doi.org/10.1109/GUCON.2018.8675049.

[5] M. Kiruthika and S. Bindu, "Classification of Electrical Power System Conditions with Convolutional Neural Networks," *Engineering, Technology & Applied Science Research*, vol. 10, no. 3, pp. 5759–5768, Jun. 2020, https://doi.org/10.48084/etasr.3512.

[6] A. G. Phadke, P. Wall, L. Ding, and V. Terzija, "Improving the performance of power system protection using wide area monitoring systems," *Journal of Modern Power Systems and Clean Energy*, vol. 4, no. 3, pp. 319–331, Jul. 2016, https://doi.org/10.1007/s40565-016-0211-x.

[7] T. B. Costa, R. O. Berriel, A. C. S. Lima, and R. F. S. Dias, "Evaluation of a Phase-Locked Loop Phasor Measurement Algorithm on a Harmonic Polluted Environment in Applications Such as PMU," *Journal of Control, Automation and Electrical Systems*, vol. 30, no. 3, pp. 424–433, Jun. 2019, https://doi.org/10.1007/s40313-019-00450-5.

[8] R. Manam and S. R. Rayapudi, "Sensitive Constrained Optimal PMU Allocation with Complete Observability for State Estimation Solution," *Engineering, Technology & Applied Science Research*, vol. 7, no. 6, pp. 2240–2250, Dec. 2017, https://doi.org/10.48084/etasr.1542.

[9] M. U. Usman and M. O. Faruque, "Applications of synchrophasor technologies in power systems," *Journal of Modern Power Systems and Clean Energy*, vol. 7, no. 2, pp. 211–226, Mar. 2019, https://doi.org/10.1007/s40565-018-0455-8.

[10] "SIPROTEC 5 Application - PMU functionality in SIPROTEC 5 devices, Edition 2," Siemens AG, APN-037, 2021.

[11] A. G. Phadke and T. Bi, "Phasor measurement units, WAMS, and their applications in protection and control of power systems," *Journal of Modern Power Systems and Clean Energy*, vol. 6, no. 4, pp. 619–629, Jul. 2018, https://doi.org/10.1007/s40565-018-0423-3.

[12] R. P. M. Silva, A. C. B. Delbem, and D. V. Coury, "Genetic algorithms applied to phasor estimation and frequency tracking in PMU development," *International Journal of Electrical Power & Energy Systems*, vol. 44, no. 1, pp. 921–929, Jan. 2013, https://doi.org/10.1016/j.ijepes.2012.07.070.

[13] S. Das, "Algorithms to Improve Performance of Wide Area Measurement Systems of Electric Power Systems," Ph.D. dissertation, University of Western Ontario, London, Canada, 2014.

[14] "IEEE Standard for Synchrophasor Data Transfer for Power Systems," *IEEE Std C37.118.2-2011 (Revision of IEEE Std C37.118-2005)*, Sep. 2011, https://doi.org/10.1109/IEEESTD.2011.6111222.

[15] H. Liu, H. Hu, H. Chen, L. Zhang, and Y. Xing, "Fast and Flexible Selective Harmonic Extraction Methods Based on the Generalized Discrete Fourier Transform," *IEEE Transactions on Power Electronics*, vol. 33, no. 4, pp. 3484–3496, Apr. 2018, https://doi.org/10.1109/TPEL.2017.2703138.

[16] D. M. Laverty, J. Hastings, D. J. Morrow, R. Khan, K. Mclaughlin, and S. Sezer, "A modular phasor measurement unit design featuring open data exchange methods," in *2017 IEEE Power & Energy Society General Meeting*, Chicago, IL, USA, Jul. 2017, pp. 1–5, https://doi.org/10.1109/PESGM.2017.8273986.

[17] M. Abbaci and M. O. Zmirli, "Performance Evaluation of PMU using Modified Cooley-Tukey Algorithm Based on GDFT," in *2018 International Conference on Applied Smart Systems (ICASS)*, Medea, Algeria, Aug. 2018, pp. 1–6, https://doi.org/10.1109/ICASS.2018.8651967.

[18] M. Shahraeini, M. S. Ghazizadeh, and M. H. Javidi, "Co-Optimal Placement of Measurement Devices and Their Related Communication Infrastructure in Wide Area Measurement Systems," *IEEE Transactions on Smart Grid*, vol. 3, no. 2, pp. 684–691, Jun. 2012, https://doi.org/10.1109/TSG.2011.2178080.

[19] X. Zhao, D. M. Laverty, A. McKernan, D. J. Morrow, K. McLaughlin, and S. Sezer, "GPS-Disciplined Analog-to-Digital Converter for Phasor Measurement Applications," *IEEE Transactions on Instrumentation and Measurement*, vol. 66, no. 9, pp. 2349–2357, Sep. 2017, https://doi.org/10.1109/TIM.2017.2700158.

[20] A. L. Kouzou, H. Bentarzi, R. D. Mohammedi, and M. Laoumer, "Optimal Placement of Phasor Measurement Unit in Power System using Meta-Heuristic Algorithms," *Electrotehnica, Electronica, Automatica*, vol. 67, no. 2, pp. 98–113, 2019.

[21] G. S. Antonova, "Phasor Data Concentrator Definitions, Functions and Standards," presented at the Hands on Relay School, Mar. 2018.

[22] R. Khan, K. McLaughlin, D. Laverty, and S. Sezer, "IEEE C37.118-2 Synchrophasor Communication Framework: Overview, Cyber Vulnerabilities Analysis and Performance Evaluation: 2nd International Conference on Information Systems Security and Privacy," *Proceedings of the 2nd International Conference on Information Systems Security and Privacy*, pp. 159–170, Feb. 2016, https://doi.org/10.5220/0005745001670178.

[23] S. G. Johnson, "Modified Cooley-Tukey algorithms based on a generalized DFT framework," 2008.

[24] H. Kim and S. Lekcharoen, "A Cooley-Tukey Modified Algorithm in Fast Fourier Transform," *Korean Journal of Mathematics*, vol. 19, no. 3, pp. 243–253, 2011, https://doi.org/10.11568/kjm.2011.19.3.243.

[25] F. Qureshi, "Optimization of Rotations in FFTs," Ph.D. dissertation, Linkoping University, 2012.

[26] H. Li, "Frequency estimation and tracking by two-layered iterative DFT with re-sampling in non-steady states of power system," *EURASIP Journal on Wireless Communications and Networking*, vol. 2019, no. 1, Art. no. 28, Feb. 2019, https://doi.org/10.1186/s13638-018-1320-1.

[27] "Report of Task Force on Testing and Certification," North American Synchrophasor Initiative Task Force (NASPI TF), Oct. 2013.